J Appl Electrochem (2007) 37:899–904
DOI 10.1007/s10800-007-9327-z

ORIGINAL PAPER

Effects of $K_4Fe(CN)_6$ on electroless copper plating using hypophosphite as reducing agent

Xueping Gan · Yating Wu · Lei Liu · Wenbin Hu

Received: 14 November 2006 / Revised: 21 March 2007 / Accepted: 23 March 2007 / Published online: 18 April 2007
© Springer Science+Business Media B.V. 2007

Abstract $K_4Fe(CN)_6$ was used to improve the microstructure and properties of copper deposits obtained from hypophosphite baths. In electroless copper plating solutions using hypophosphite as the reducing agent, nickel ions (0.0038 M with Ni^{2+}/Cu^{2+} mole ratio 0.12) was used to catalyze hypophosphite oxidation. However, the color of the copper deposits was dark or brown and its resistivity was much higher than that obtained in formaldehyde baths. The effects of $K_4Fe(CN)_6$ on the deposit composition, resistivity, structure, morphology and the electrochemical reactions of hypophosphite (oxidation) and cupric ion (reduction) have been investigated. The deposition rate and the resistivity of the copper deposits decreased significantly with the addition of $K_4Fe(CN)_6$ to the plating solution and the color of the deposits changed from dark-brown to copper-bright with improved uniformity. The nickel and phosphorus content in the deposits also decreased slightly with the use of $K_4Fe(CN)_6$. Smaller crystallite size and higher (111) plane orientation were obtained by addition of $K_4Fe(CN)_6$. The electrochemical current–voltage results show that $K_4Fe(CN)_6$ inhibited the catalytic oxidation of hypophosphite at active nickel sites and reduced the reduction reaction of cupric ions on the deposit surface by adsorption on the electrode. This results in lower deposition rate and a decrease in the mole ratio of $NaH_2PO_2/CuSO_4$ consumed during plating.

X. Gan · Y. Wu · L. Liu · W. Hu (✉)
State Key Laboratory of Metal Matrix Composites, Shanghai Jiao Tong University, Shanghai 200030, China
e-mail: material_hu@163.com

X. Gan
e-mail: ganxueping@sjtu.edu.cn

Keywords $K_4Fe(CN)_6$ · Hypophosphite · Electroless copper plating · Copper deposits

1 Introduction

Electroless copper deposition technology has advanced rapidly in recent years including widespread application in areas such as through-hole plating in printed circuit boards, decorative plating of household utensils and in the automotive industry, electromagnetic interference shielding of electronic components, conductive traces in electronic interconnection devices and integrated circuit manufacturing [1–3]. Commercial electroless copper plating solutions often use formaldehyde or its derivatives as reducing agents and are operated at pH values above 11 [4]. Furthermore, it has been found that this bath may release hazardous gases during operation [5]. Therefore, previous paper has investigated electroless copper solutions using nonformaldehyde reducing agents such as dimethylamine borane (DMBA) [6], sodium hypophosphite [7, 8], and cobalt(II)-ethylenediamine complex [9]. Among these, sodium hypophosphite is especially attractive because of its low pH, low cost and relative safety [10, 11]. However, the hypophosphite-based electroless copper plating process is complicated because copper is not a good catalyst for the oxidation of hypophosphite resulting in little or no plating on a pure copper surface. One approach to catalyze the oxidation of the reducing agent is to add nickel ions (or other metal ions) to the bath, resulting in a very small amount of co-deposited nickel in the copper deposit. The nickel serves to catalyze the oxidation of hypophosphite enabling continuous copper deposition [11]. When the $Ni^{2\Downarrow}/Cu^{2\Downarrow}$ ← mole ratio in the bath was low, the deposition rate of the copper plating decreased with time and

finally stopped because the surface catalytic activity was not replenished. Thus, it was necessary to maintain the $Ni^{2\Downarrow}/Cu^{2\Downarrow} \leftarrow$ mole ratio above a critical value to sustain the deposition rate. However, the copper deposit properties were degraded and the deposit appearance became darker with increased $Ni^{2\Downarrow}/Cu^{2\Downarrow} \leftarrow$ mole ratio. Consequently it is important to improve the microstructure and properties of the copper deposit while maintaining the nickel(II) concentration in the bath.

$K_4Fe(CN)_6$ has been used as stabilizer or brightener in formaldehyde-based electroless copper plating baths to improve the physical properties of the copper deposits [12, 13]. In this study, the influence of $K_4Fe(CN)_6$ on the hypophosphite-based electroless copper process has been investigated. The composition, microstructure and properties of the copper deposits obtained at different $K_4Fe(CN)_6$ concentrations in the bath are reported along with voltametric analysis of its role.

2 Experimental

Polyethylene terephthalate (PET) boards (area: 25 cm^2) were used as the substrates for the electroless copper plating.

Electroless plating was carried out by a multi-step processes, which included: scouring, rinsing, etching, rinsing, sensitization, rinsing, activation, electroless copper plating, rinsing and drying. The specimens were scoured in 5.0 g L^{-1} NaOH solution at 70 °C for 5 min prior to use. The samples were rinsed then in distilled water and etched in a mixture of 15 g L^{-1} $KMnO_4$ and 40 mL L^{-1} H_2SO_4 solution for 5 min. Surface sensitization was conducted by immersion of the samples into an aqueous solution containing 10 g L^{-1} $SnCl_2$ and 40 mL L^{-1} 38% HCl at 30 °C for 5 min. The specimens were then rinsed in distilled water and immersed in an activator containing 0.50 g L^{-1} $PdCl_2$ and 20 mL L^{-1} 38% HCl at 40 °C for 5 min. The specimens were then rinsed in a large volume of deionized water for more than 5 min to prevent contamination of the plating bath. The specimens were then immersed in the electroless copper plating bath for 30 min. The electroless copper plating bath contained: 0.032 M $CuSO_4{\cdot}5H_2O$, 0.0038 M $NiSO_4{\cdot}7H_2O$, 0.283 M $NaH_2PO_2{\cdot}H_2O$, 0.071 M $H_3C_6H_5O_7{\cdot}H_2O$, 0.493 M HBO_3 and 0–6 ppm $K_4Fe(CN)_6$. Deionized water was used to prepare the solutions. The pH was adjusted using NaOH or H_2SO_4 to a final value of 9.5 ± 0.1. The temperature was held at 70 ± 1 °C. Finally, the samples were rinsed with distilled water and ethyl alcohol and dried in an oven at 55 °C.

Copper deposition rates were determined by the change in weight of the PET boards after plating assuming uniform plating and the mass density of copper to be 8.92 g cm^{-3}. The resistivity of the copper deposits were measured using the four-point probe method as described in ASTM F390. The crystal structure of the copper deposits was investigated using X-ray diffraction (XRD, Cu Kα radiation and graphite filter at 40 kV and 100 mA). Scanning electron microscopy (SEM, JEOL JSM-6460) was used to characterize the surface morphology of the deposits. The chemical composition of the copper deposits was determined using energy dispersive X-ray (EDX) analysis attached to the SEM. The concentration of $CuSO_4$ and NaH_2PO_2 before and after plating was measured by chemical analysis.

A PARSTAT model 2273 potentiostat was used for electrochemical measurements. Linear sweep voltammetry (LSV) experiments were carried out at 70 °C and at a scan rate of 10 mV s^{-1}. The working electrode was pure copper of 1.0 cm^2 surface area; the counter electrode was a platinum foil and the reference electrode was a commercial Ag/AgCl electrode saturated with KCl. Prior to each test the electrodes were immersed in the electrolyte until a steady open circuit potential (OCP) was reached.

3 Results and discussion

3.1 Deposition rate

The effect of $K_4Fe(CN)_6$ concentration in plating solutions on the deposition rate is shown in Fig. 1. The nickel ion concentration in the bath was 0.0038 M and the Ni^{2+}/Cu^{2+} mole ratio was 0.12. The deposition rate of the electroless plating in the absence of $K_4Fe(CN)_6$ was high and the deposits were dark brown. $K_4Fe(CN)_6$ had an obvious effect on the copper deposition rate. The deposition rate decreased from 11 to 4 μm h^{-1} (as measured after 30 min plating) as the concentration of $K_4Fe(CN)_6$ was increased from 0 to 4 ppm. There was little difference in deposition rate at higher $K_4Fe(CN)_6$ concentration. It is possible that

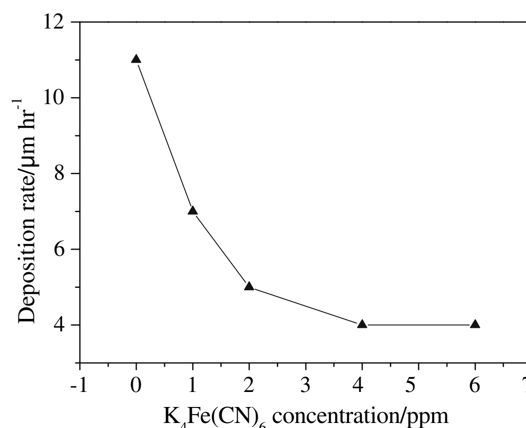

Fig. 1 The effect of $K_4Fe(CN)_6$ concentration on deposition rate

the reduction in the deposition rate with the addition of $K_4Fe(CN)_6$ results from its adsorption on the electrode surface causing a lower rate of electron transfer or nucleation. The effect slows with further addition of $K_4Fe(CN)_6$ as the surface adsorption reaches saturation. In addition, the $K_4Fe(CN)_6$ probably interacts with Cu(II)-Citrate complex forming weak mixed complex $[Cu_2YFe(CN)_6]^{3-}$ ($Y = C_6H_5O_7^{3-}$).

3.2 Surface morphology

The surface morphology of the copper deposits was studied by scanning electron microscopy (SEM). SEM photographs of the surface of copper deposits obtained at different $K_4Fe(CN)_6$ concentration are shown in Fig. 2. Figure 2a shows that the copper deposits were loose or porous and the topography was rough in the absence of $K_4Fe(CN)_6$. The copper crystal grains grew only vertical to the substrate surface, which resulted in porous deposits and high resistivity. The deposits became compact and the topography became smooth with the addition of $K_4Fe(CN)_6$. Figure 2b–d show that the grain size decreased slightly as the concentration of $K_4Fe(CN)_6$ increased from 1 to 4 ppm. The color of the deposits also had a corresponding improvement, changing from dark-brown to copper-bright with increase in $K_4Fe(CN)_6$ concentration. The bright appearance of the deposits usually indicates better mechanical and physical properties.

3.3 Composition and microstructure

The composition at the surface of the copper deposits as a function of $K_4Fe(CN)_6$ concentration was investigated using energy dispersive X-ray analysis. The deposits consisted mainly of copper with a small amount of nickel and phosphorus as given in Table 1. The total content of nickel and phosphorus was 3–5 wt% and decreased slightly with increase in $K_4Fe(CN)_6$ concentration. Nickel ions are required in the hypophosphite-based electroless copper plating bath to maintain the deposition rate. Nickel catalytically participates in the oxidation of hypophosphite. The copper deposition rate increased with nickel ion concentration [11].

The XRD patterns of the copper deposits obtained at different $K_4Fe(CN)_6$ concentrations are shown in Fig. 3. The peaks appearing at 2θ = 43.3°, 50.5°, 74.2°, and 89.9° represent (111), (200), (220) and (311) planes, respectively. The copper oxide phase was not detected in the deposits. The effective crystallite size of the copper deposits can be estimated from the broadening of the diffraction peak from the (111) planes by the use of Scherrer's equation [14, 15]:

$$D = \frac{0.89\lambda}{\beta_{1/2}\cos\theta}$$

where λ is the wavelength of Cu Kα, $\beta_{1/2}$ the half width of diffraction line and θ the diffraction angle. The calculated effective crystallite size of the copper deposits and relative intensities of the diffraction peaks from the (111), (200), (220) and (311) planes are listed in Table 2. It can be seen that the copper deposit has a decreased crystallite size and intensified (111) plane orientation with the addition of $K_4Fe(CN)_6$ to the plating bath.

3.4 Resistivity

In the bath without addition of $K_4Fe(CN)_6$, the copper deposition rate was very high resulting in large crystallite

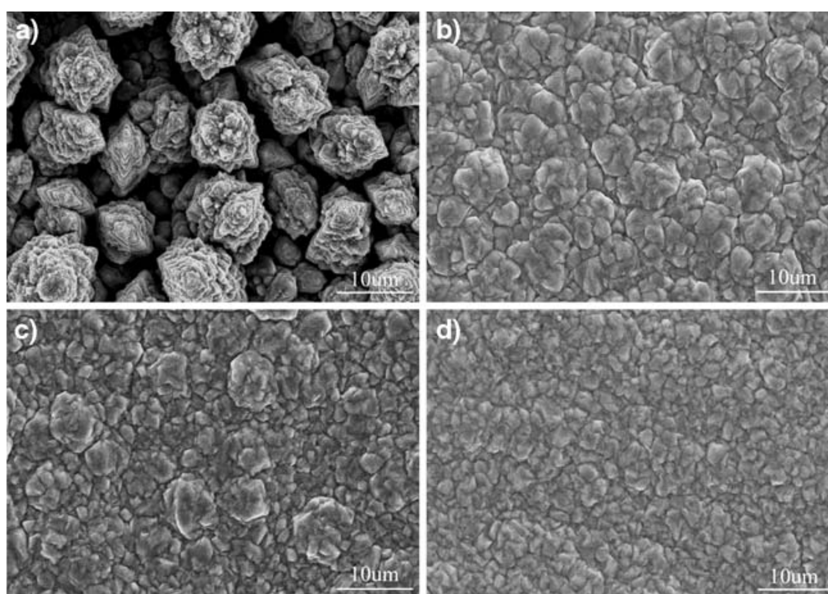

Fig. 2 SEM photographs of the deposits surface obtained at different $K_4Fe(CN)_6$ concentration bath: (**a**) 0 ppm; (**b**) 1 ppm; (**c**) 2 ppm; (**d**) 4 ppm

Table 1 The nickel and phosphorus content in the copper deposits from the bath with different $K_4Fe(CN)_6$ concentrations

Copper deposits	$K_4Fe(CN)_6$ concentration/ ppm	Ni + P/P content/ wt%
1	0	4.88/0.43
2	1	4.46/0.40
3	2	3.93/0.36
4	4	3.34/0.30

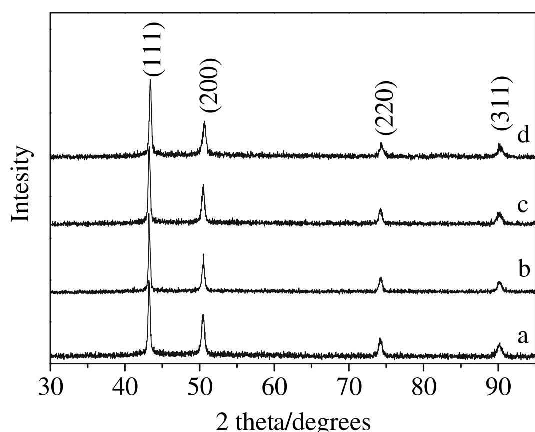

Fig. 3 The XRD patterns of the copper deposits obtained at different $K_4Fe(CN)_6$ concentration :(**a**) 0 ppm; (**b**) 1 ppm; (**c**) 2 ppm; (**d**) 4 ppm

Table 2 Characteristic peak relative intensities and crystallite size of the copper deposits from the bath with different $K_4Fe(CN)_6$ concentrations

$K_4Fe(CN)_6$ concentration /ppm	Crystallite size /nm	I(111)	I(200)	I(220)	I(311)
0	5.891	100	59	29	23
1	5.891	100	51	28	22
2	5.236	100	51	25	20
4	4.713	100	50	23	20

with poor microstructure due to the rapid nucleation and growth [13]. This poor microstructure is consistent with a loose or porous copper deposit observed when $K_4Fe(CN)_6$ was absent from the bath. Consequently, the poor quality copper deposits produced in the absence of $K_4Fe(CN)_6$ have much higher resistivity. The resistivity of the as-plated copper deposits versus $K_4Fe(CN)_6$ concentration is shown in Fig. 4. By adding 1 ppm $K_4Fe(CN)_6$ to the solution, the resistivity of the copper deposits decreased significantly because the copper deposits became more compact. There is little difference in resistivity with higher $K_4Fe(CN)_6$ concentration. It can be seen that the resistivity of the copper deposits were all higher than those deposited from formaldehyde-based electroless copper plating baths (2.0–3(0 μm h^{-1}) [16], which can be explained by the fact that Ni–P alloy has high electrical resistivity (120 ≈ Ω cm) [17] and the nickel atoms in the copper lattice increase the number of crystal defects in the copper deposit.

3.5 Liner sweep voltammetry

According to the mixed potential theory of electroless plating [18], the overall reaction is determined by the two half-reactions on the same electrode, i.e. the reduction of cupric ions and the oxidation of the reducing agent. Consequently, studying the effects of $K_4Fe(CN)_6$ on the half-reactions can help understand the role of $K_4Fe(CN)_6$ in the electroless copper plating bath.

Figure 5 shows the LSV (from OCP positively to 0.10 V) for hypophosphite oxidation on copper in an electrolyte containing 0.283 M sodium hypophosphite, 0.071 M sodium citrate, 0.493 M boric acid and 0.0038 M nickel sulfate. The oxidation of hypophosphite was lowered by addition of $K_4Fe(CN)_6$ resulting in an obvious decrease in the oxidation current. This shows that $K_4Fe(CN)_6$ increased the overpotential for the oxidation of hypophosphite. The reduction of cupric ions was also investigated versus $K_4Fe(CN)_6$ concentration by LSV in an electrolyte containing 0.032 M CuSO4 · 5H2O, 0.051 M sodium citrate, 0.493 M boric acid, 0.0038 M nickel sulfate, as shown in Fig. 6. The addition of 1 ppm (or greater) $K_4Fe(CN)_6$ caused only a small decrease in the cathodic current. There was little difference in the cathodic current at higher $K_4Fe(CN)_6$ concentrations. According to Figs. 5 and 6 it can be suggested that the overall decrease in deposition rate is mainly due to delayed oxidation of hypophophite and not by copper ion reduction, which is consistent with other results [19].

The main overall reaction for electroless copper using hypophosphite as reducing agent is:

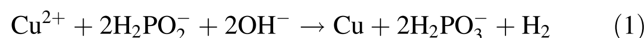

$$Cu^{2+} + 2H_2PO_2^- + 2OH^- \rightarrow Cu + 2H_2PO_3^- + H_2 \quad (1)$$

The mole ratio of $NaH_2PO_2/CuSO_4$ in this reaction is 2. Besides this reaction, there is a side reaction consuming hypophosphite and evolving hydrogen gas [20]:

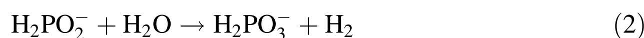

$$H_2PO_2^- + H_2O \rightarrow H_2PO_3^- + H_2 \quad (2)$$

Therefore, the mole ratio of $NaH_2PO_2/CuSO_4$ consumed during plating must be more than 2. The effect of $K_4Fe(CN)_6$ on the mole ratio of $NaH_2PO_2/CuSO_4$ was also investigated. The mole ratio of $NaH_2PO_2/CuSO_4$ at different $K_4Fe(CN)_6$ concentration is listed in Table 3. The mole ratio of $NaH_2PO_2/CuSO_4$ decreased from 7 to 3.5 as

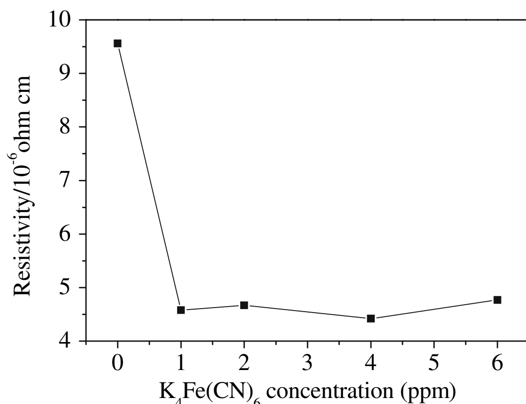

Fig. 4 The influence of $K_4Fe(CN)_6$ concentration on the resistivity of copper deposits

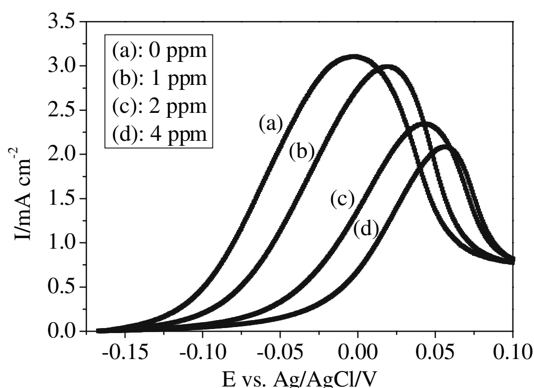

Fig. 5 Current–potential curves for the oxidation of hypophosphite with different $K_4Fe(CN)_6$ concentrations in the electrolyte containing 0.283 M $NaH_2PO_2 \cdot H_2O$, 0.071 M $H_3C_6H_5O_7 \cdot H_2O$, 0.493 M HBO_3 and 0.0038 M $NiSO_4 \cdot 7H_2O$

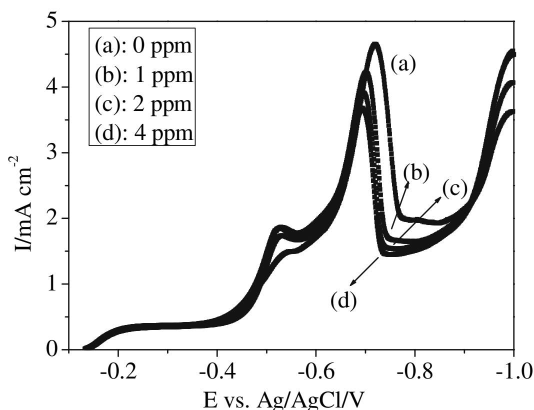

Fig. 6 Current–potential curves for the reduction of cupric ion with different $K_4Fe(CN)_6$ concentrations in the electrolyte containing 0.032 M $CuSO_4 \cdot 5H_2O$, 0.0038 M $NiSO_4 \cdot 7H_2O$, 0.071 M $H_3C_6H_5O_7 \cdot H_2O$ and 0.493 M HBO_3

Table 3 The mole ratio of $NaH_2PO_2/CuSO_4$ consumed during plating at different $K_4Fe(CN)_6$ concentration

$K_4Fe(CN)_6$ concentration /ppm	0	1	2	4
Mole ratio of $NaH_2PO_2/CuSO_4$	7	5.2	4.2	3.5

the $K_4Fe(CN)_6$ concentration increased from 0 to 4 ppm, which directly indicates that the addition of $K_4Fe(CN)_6$ lowered the rate of the side reaction during plating and also reduced consumption of hypophosphite.

4 Conclusions

$K_4Fe(CN)_6$ improves the microstructure and properties of copper deposits obtained from electroless copper plating using hypophosphite as reducing agent. With the addition of $K_4Fe(CN)_6$ to the plating bath containing 0.0038 M nickel ions, the color of the deposit changed from dark-brown to copper-bright and the deposits became uniform and compact. The deposits had a smaller crystallite size and higher (111) plane orientation with the addition of $K_4Fe(CN)_6$. The electroless deposition rate and resistivity of the copper deposits decreased significantly with addition of $K_4Fe(CN)_6$. However, the resistivity of the deposits was higher than that of deposits from formaldehyde-based electroless copper plating due to the presence of nickel. The nickel and phosphorus content in the deposits decreased slightly with addition of $K_4Fe(CN)_6$. The LSVs showed that $K_4Fe(CN)_6$ inhibited the catalytic oxidation of hypophosphite most probably at active nickel sites and reduced the reduction reaction of cupric ions on the deposit surface by adsorption on the electrode. This resulted in a lower deposition rate and a decrease in the mole ratio of $NaH_2PO_2/CuSO_4$ consumed during plating.

References

1. Kou SC, Hung A (2003) Plat Surf Finish 90(3):44
2. Deckert CA (1995) Plat Surf Finish 82(2):48
3. Deckert CA (1995) Plat Surf Finish 82(2):58
4. Li J, Kohl PA (2003) J Electrochem Soc 150(8):C558
5. Cheng DH, Xu WY, Zhang ZY, Yiao ZH (1997) Met Finish 95(1):34
6. Rangarajan J, Mahadevaiyer K, Gregory W (1989) U.S. Pat. 4,818,286
7. Hung A, Ohno I (1990) J Electrochem Soc 137(3):918
8. Hung A, Chen KM (1989) J Electrochem Soc 136(1):72
9. Vaskelis A, Norkus E, Jaciauskiene J (2002) J Appl Electrochem 32:297
10. Li J, Kohl PA (2002) J Electrochem Soc 149(12):C631
11. Li J, Hayden H, Kohl PA (2004) Electrochim Acta 49:1789
12. Lin WH, Chang HF (1998) Surf Coat Technol 107:48
13. Vaskelis A, Jaciauskiene J, Stalnioniene I, Norkus E (2006) J Electroanal Chem 600(1):6

14. Cullity BD (1978) Elements of X-ray Diffraction. Addison-Wesley, London
15. Fierro JLF (1990) Spectroscopic characterization of heterogeneous catalysts, part: B. Elsevier, The Netherlands
16. Patterson JC, O'Reilly M, Crean GM, Barrett J (1997) Microelectron Eng 33:65
17. Tzeng SS, Chang FY (2001) Thin Solid Films 388:143
18. Ohno I, Wakabayashi O, Haruyama S (1985) J Electrochem Soc 132:2323
19. Paunovic M, Zeblisky R (1985) Plat Surf Finish 72(2):52
20. Hung A (1988) Plat Surf Finish 75(1):62